Small-signal ac conductivity and velocity overshoot in semiconductor materials

S. Teitel[a] and J. W. Wilkins
Laboratory of Atomic and Solid State Physics, Cornell University, Ithaca, New York 14853

(Received 17 December 1981; accepted for publication 12 March 1982)

We consider the response of a semiconductor to small perturbations in the applied electric field away from a steady uniform dc field. Both ac conductivity and time-dependent velocity response are calculated for a relaxation model described by moment equations for the average electron velocity and energy. Our model involves only three parameters determined by the energy and momentum relaxation rates and their derivatives. Two of them, the momentum relaxation rate Γ_m which sets the frequency and time scales and the ratio $(dJ/dE)/(J/E)$, are easily obtained from dc conductivity measurements. The third can be obtained from a measurement of the value of the peak ac conductivity in the case where the peak occurs at a nonzero frequency. The form of the conductivity is explored as a function of these parameters, and consistency tests are suggested to determine the applicability of the model. The cutoff frequency where the ac conductivity drops to half its zero-frequency value is shown to be determined largely by the dc parameters Γ_m and $(dJ/dE)/(J/E)$. Precise restrictions on the parameters are given for the existence of velocity overshoot in the presence of the dc bias field. It is shown that observation of a peak ac conductivity at a nonzero frequency always implies the presence of velocity overshoot. The cutoff frequency for a spatially uniform system is shown to be insensitive to the presence of velocity overshoot.

PACS numbers: 72.20.Ht,72.30. + q,72.20.Fr

I. INTRODUCTION

The frequency dependence of the electrical conductivity in the presence of a bias dc field has long been a means of investigating hot electron effects in semiconductor materials.[1,2] The effect of velocity overshoot has been of interest as a means of improving semiconductor-device performance.[3–5] In this paper we discuss these two phenomena and the relationship between them by considering the time dependence of the average electron velocity and energy for a spatially uniform system in response to small perturbations in the applied electric field E, away from a steady dc value E_0.

In Sec. II we discuss the relaxation approximation we will use in subsequent calculations. Our model will be limited to those cases where conduction takes place primarily in only one set of equivalent conduction valleys. The response of the system to small perturbations is shown to be entirely specified by three parameters determined from the energy and momentum relaxation rates.

In Sec. III we consider the case where the perturbation E_1 is a small oscillation of frequency ω. The resulting frequency-dependent conductivity $\sigma(\omega, E_0)$ is discussed. Precise restrictions on the parameters of the theory are given in order to see an increasing conductivity at low frequencies (i.e., a peak conductivity at a finite frequency). The magnitude and frequency of peak conductivity are given as functions of these parameters. The cutoff frequency, where $\sigma(\omega, E_0)$ drops to half its zero frequency value, is also shown as a function of these parameters. It is shown how a dc measurement uniquely determines two of the parameters of the model and how an ac measurement can determine the third for certain cases of interest. Comparison with recent experiments is made.

In Sec. IV we consider the case where E_1 is a small step applied at $t = 0$. By computing how the average velocity rises to its steady-state value corresponding to the field $E_0 + E_1$, the possibilities for velocity overshoot are investigated. By velocity overshoot we mean that at short times the average velocity exceeds the final steady-state value. Precise restrictions on the parameters of the theory are given for velocity overshoot to exist. The magnitude of the overshoot and the time at which the peak velocity occurs are given as a function of these parameters. By comparison with the results of the previous section we show that, for the same dc bias field E_0, the existence of the velocity overshoot can always be inferred by the observation of a peak conductivity at a finite frequency, but that such a conductivity is not necessary for the existence of velocity overshoot. We also show that the existence of velocity overshoot does not significantly alter the cutoff frequency of the conductivity for a uniform system.

In Sec. V we summarize our conclusions.

II. RELAXATION APPROXIMATION

To describe the time evolution of the average electron velocity v and energy ϵ we start with a commonly used[6–11] relaxation model given by the following moment equations:

$$\frac{dv}{dt} = \frac{qE}{m} - v\Gamma_m(\epsilon), \tag{1a}$$

$$\frac{d\epsilon}{dt} = qEv - (\epsilon - \epsilon_L)\Gamma_e(\epsilon), \tag{1b}$$

where q is the electronic charge, m is the effective electron mass (parabolic dispersion is assumed), and ϵ_L is the equilib-

[a] Present address: Department of Physics, The Ohio State University, Columbus, Ohio 43210.

 0021-8979/82/075006-07$02.40

rium lattice thermal energy. The approach to steady state is determined by the momentum and energy relaxation rates Γ_m and Γ_e, which are assumed to be instantaneous functions of ϵ (such a model is usually viewed as arising from the assumption of a displaced Maxwellian distribution[6]). We will subsequently solve a linearized version of these equations for the case of small perturbations about the steady state.

The above equations describe the case where the conduction electrons occupy just one set of equivalent conduction valleys. Such is the case for bulk Si or Ge. Equations (1) should also apply in the case of inversion layers where the temperature is so low that only the lowest quantized level is significantly populated. Such is the case in recent experiments reported by Allen *et al.*[12] For materials such as GaAs or InP, where significant conduction takes place in higher-mass satellite valleys, Eqs. (1) are not adequate. One must introduce separate equations for each valley with appropriate transfer rates coupling them.[6,13] Others have tried to simulate such materials using Eqs. (1) with an energy-dependent mass $m(\epsilon)$.[8] We confine ourselves to the single-valley case with a constant m.

The relaxation rates $\Gamma_m(\epsilon)$ and $\Gamma_e(\epsilon)$ which appear in Eqs. (1) are uniquely determined by a knowledge of the steady-state solutions v_0 and ϵ_0 as functions of the applied electric field E.[11] Since (1) gives for the steady state

$$v_0 = \frac{qE}{m\Gamma_m}, \tag{2a}$$

$$\epsilon_0 = \frac{qEv_0}{\Gamma_e} + \epsilon_L, \tag{2b}$$

knowledge of $v_0(E)$ and $\epsilon_0(E)$ enables the determination of the relaxation rates as a function of E, i.e., $\Gamma_m(E)$ and $\Gamma_e(E)$. Inversion of the function $\epsilon_0(E)$ then gives the rates as functions of energy. Although one may question the validity of trying to explain transient phenomena with a model completely determined by its steady-state solutions, previous calculations[10,11] have shown reasonable agreement between the model represented by (1) and the transient behavior seen in more exact Monte Carlo calculations. In this paper we assume the correctness of the model and examine its consequences.

For small perturbations in the electric field, we can expand Eqs. (1) about the steady state by writing

$$E(t) = E_0 + E_1(t), \tag{3a}$$

$$v(t) = v_0 + v_1(t), \tag{3b}$$

$$\epsilon(t) = \epsilon_0 + \epsilon_1(t), \tag{3c}$$

$$\Gamma[\epsilon(t)] = \Gamma(\epsilon_0) + \left(\frac{d\Gamma}{d\epsilon_0}\right)\epsilon_1(t) + 0(\epsilon_1^2), \tag{3d}$$

where the subscript 0 denotes the steady-state solution given by (2), and the subscript 1 denotes the deviation from it. Substituting (3) into Eq. (1), linearizing in the deviations from steady state, and rewriting in dimensionless form, we find

$$\frac{d\tilde{v}}{d\tilde{t}} = \frac{E_1}{E_0} - \tilde{v} - G_m\tilde{\epsilon}, \tag{4a}$$

$$\frac{d\tilde{\epsilon}}{d\tilde{t}} = \frac{E_1}{E_0} + \tilde{v} - G_e\tilde{\epsilon}, \tag{4b}$$

where the dimensionless quantities are defined as

$$\tilde{v} \equiv v_1/v_0, \quad \tilde{\epsilon} \equiv \epsilon_1\Gamma_{m0}/(\epsilon_0 - \epsilon_L)\Gamma_{e0},$$

and

$$\tilde{t} \equiv \Gamma_{m0}\, t \quad [\Gamma_0 \equiv \Gamma(\epsilon_0)]. \tag{4c}$$

Equations (4) involve only two unknown parameters:

$$G_m \equiv (\epsilon_0 - \epsilon_L)\frac{\Gamma_{e0}}{\Gamma_{m0}^2}\left(\frac{d\Gamma_m}{d\epsilon}\right)_0 \tag{5a}$$

$$G_e \equiv \frac{1}{\Gamma_{m0}}\left(\frac{d(\epsilon - \epsilon_L)\Gamma_e}{d\epsilon}\right)_0, \tag{5b}$$

which characterize the energy dependence of the relaxation rates. [From Ref. 10, where Γ_m and Γ_e are computed for Si, we can expect G_e and G_m to be $<0(10)$.] Equations (4), the definition $v \equiv v_1/v_0$, and Eq. (2a) for v_0 show that, to completely specify the velocity response $v_1(t)$, all that remains to be known in addition to G_e and G_m is the relaxation rate Γ_{m0}. In the remaining section we explore the behavior of solutions to Eq. (4) as a function of the three parameters G_m, G_e, and Γ_{m0}

III. ac CONDUCTIVITY

To extract the complex ac electrical conductivity $\sigma(\omega,E_0)$ from Eqs. (4), we assume that all quantities have the time dependence $\exp(i\omega t)$ and use the definition

$$\sigma(\omega,E_0) = nqv_1/E_1, \tag{6}$$

where n is the conduction electron density.

The resulting conductivity, as previously derived by Das and Ferry,[7] is in our notation,

$$\frac{\sigma(\omega,E_0)}{\sigma_{dc}(E_0)} = \frac{G_e - G_m + i\tilde{\omega}}{(G_e + i\tilde{\omega})(1 + i\tilde{\omega}) + G_m}, \tag{7}$$

where $\tilde{\omega} \equiv \omega/\Gamma_{m0}$ is the dimensionless frequency and $\sigma_{dc}(E_0) \equiv nqv_0/E_0$ is the dc conductivity. From Eq. (2a) for v_0, we have the familiar result

$$\sigma_{dc}(E_0) = nq^2/m\Gamma_{m0}. \tag{8}$$

Knowledge of the conduction electron density n and the dc conductivity thus suffices to determine Γ_{m0}.

We stress the difference between the dc conductivity $\sigma_{dc}(E_0)$ and the zero frequency limit of the ac conductivity $\sigma(\omega = 0,E_0)$ in Fig. 1. Plotted is a typical curve of the dc

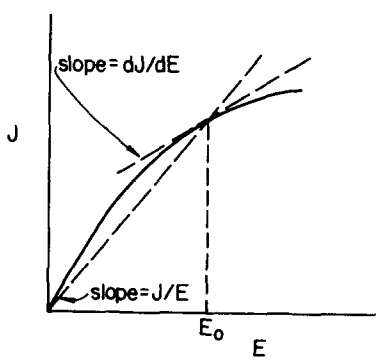

FIG. 1. dc current J vs electric field E. dc conductivity $\sigma_{dc}(E) = J/E$ and zero frequency ac conductivity $\sigma(\omega = 0,E) = dJ/dE$ are given by the slopes of the appropriately labeled lines.

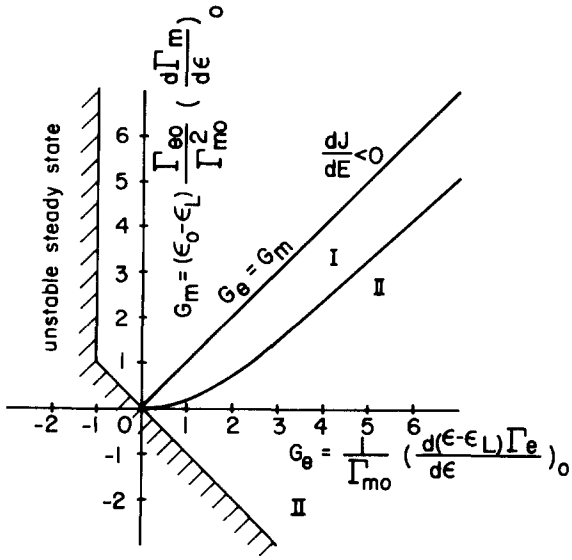

FIG. 2. Division of G_m and G_e parameter space according to behavior of ac conductivity. For points in region I, $\mathrm{Re}[\sigma(\omega,E_0)]$ rises at low ω, reaches a peak at some $\omega_{\mathrm{peak}} \neq 0$, and then decays to zero. For points in region II, $\mathrm{Re}[\sigma(\omega,E_0)]$ decrease monotonically as ω increases. Above the line $G_e = G_m$ there is negative differential conductivity, i.e., $\sigma(\omega = 0,E) = (dJ/dE) < 0$. To the left of the hatched line the steady state is unstable.

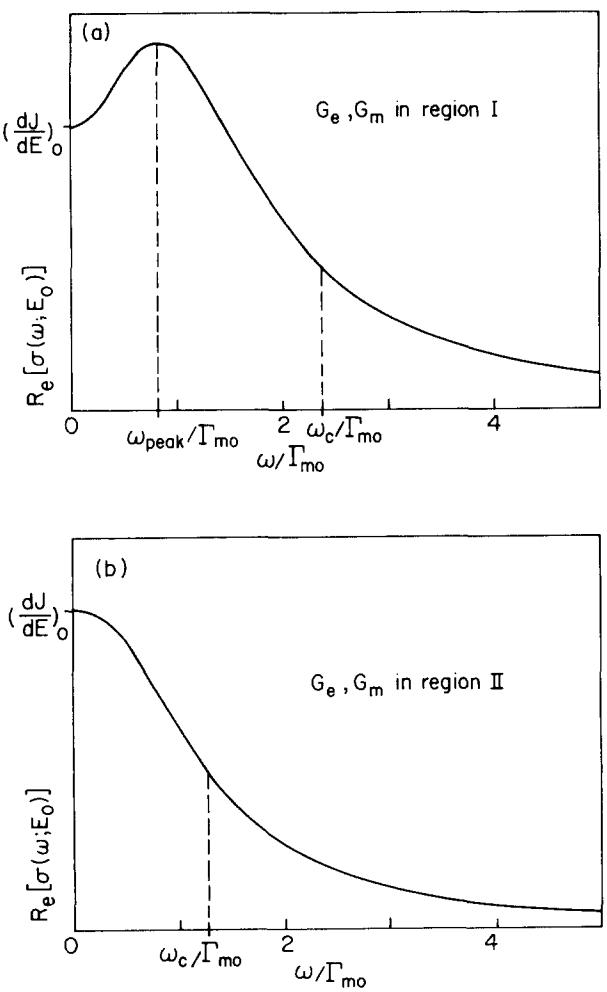

FIG.3. Typical plots of $\mathrm{Re}[\sigma(\omega,E)]$ as a function of ω/Γ_{m0}. Plot (a) corresponds to values of G_e and G_m in region I of Fig. 2, while plot (b) corresponds to values of G_e and G_m in region II of Fig. 2.

current J versus field E. $\sigma_{\mathrm{dc}}(E_0)$ is just the chordal value J/E, while $\sigma(\omega = 0,E_0)$ is the differential value dJ/dE. The ratio of these two values is given by the zero frequency limit of Eq. (7) as

$$\frac{\sigma(\omega = 0,E_0)}{\sigma_{\mathrm{dc}}(E_0)} = \left(\frac{dJ/dE}{J/E}\right)_0 = \frac{G_e - G_m}{G_e + G_m}. \tag{9}$$

Since this ratio is directly measurable by a simple dc experiment while G_e and G_m separately are not, it will be convenient later to regard Eq. (9), instead of G_m, as one of the three fundamental parameters of the system. G_m can then be determined from Eq. (9) once $(dJ/dE)/(J/E)$ and G_e are known.

The ac conductivity (7) displays various possible behavior depending on the values of G_e and G_m. In Fig. 2 we divide this parameter space into distinct regions, and in Fig. 3 we show typical plots of $\mathrm{Re}[\sigma(\omega,E_0)]$ for the two main regions of interest. In region I the conductivity increases at low frequencies, reaches a peak value at some frequency ω_{peak}, and then decays to zero as $1/\omega^2$. In region II the conductivity decreases as ω increases, and the curve looks roughly like the Drude model given by $\sigma(\omega)/\sigma_{\mathrm{dc}} = 1/(1 + i\omega/\Gamma_m)$.

Note that the region of parameter space $G_e < -1$ or $G_m < -G_e$ is not permitted. For values of G_e and G_m in this region, the homogenous solutions to Eq. (4) grow rather than decay exponentially in time, and hence the steady state is unstable. Exclusion of this region insures that all poles of the conductivity $\sigma(\omega,E)$ remain in the upper-half of the complex ω plane and hence causality is preserved. We have also not considered the region $G_m > G_e$ as this is a region of negative differential conductivity, i.e., $dJ/dE < 0$ [see Eq. (9)]. Since negative differential conductivity is usually associated with a transfer of electrons to higher-mass satellite valleys,[14]

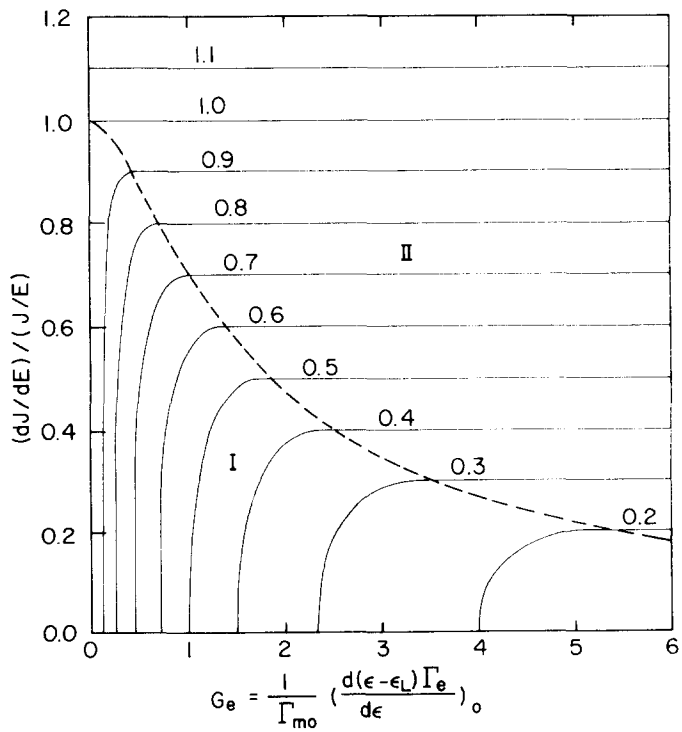

FIG. 4. Contours of peak conductivity $\mathrm{Re}[\sigma(\omega_{\mathrm{peak}},E_0)]/\sigma_{\mathrm{dc}}(E_0)$ as a function of $(dJ/dE)/(J/E)$ and G_e. Below the dashed line corresponds to region I of Fig. 2, while region II of Fig. 2 is above.

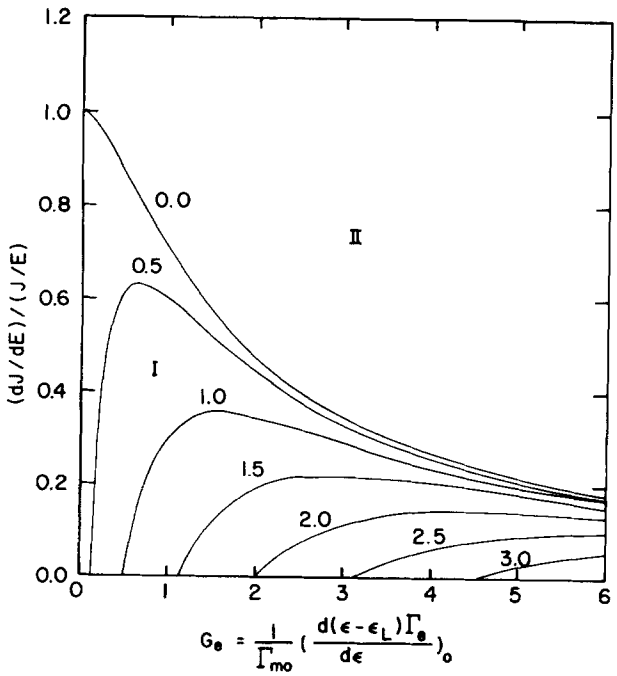

FIG. 5. Contours of frequency of peak conductivity $\omega_{peak}/\Gamma_{m0}$ as a function of $(dJ/dE)/(J/E)$ and G_e. The contour $\omega_{peak} = 0$ separates the regions I and II of Fig. 2 [in region II, $\omega_{peak} = 0$ for all values of $(dJ/dE)/(J/E)$ and G_e].

the one-valley model implicit in Eqs. (1) is probably inadequate for an accurate description in this region.

We have previously remarked how two of the three parameters of the system, Γ_{m0} and $(dJ/dE)/(J/E)$, are readily measurable by a dc experiment. We now show how the third parameter G_e can be obtained for the case of region I. In Fig. 4 we plot contours of peak conductivity $\mathrm{Re}[\sigma(\omega_{peak}, E_0)]$ as a function of the parameters $(dJ/dE)/(J/E)$ and G_e. The region below the dashed line represents the region I of Fig. 2 while the region II lies above. From Fig. 4 it is easily seen that, in region I, a measurement of $\mathrm{Re}[\sigma(\omega_{peak}, E_0)]$ is sufficient to determine G_e and complete the specification of the behavior of the system. G_e is uniquely determined by the intersection of the measured value $(dJ/dE)/(J/E)$ with the contour of the measured value $\mathrm{Re}[\sigma(\omega_{peak}, E_0)]/\sigma_{dc}$. G_m can then be obtained from Eq. (9), and the complete frequency dependence of $\sigma(\omega, E_0)$ may be plotted from Eq. (7).

Similarly, in Fig. 5 we plot contours of $\omega_{peak}/\Gamma_{m0}$ A measurement of just ω_{peak} does not necessarily determine G_e uniquely. For example, the contour for $\omega_{peak}/\Gamma_{m0} = 0.5$ has two possible values of G_e for the value $(dJ/dE)/(J/E) = 0.4$. However, a measurement of both $\sigma(\omega_{peak}, E_0)$ and ω_{peak} must be able to give a consistent value for G_e. Such a consistency test provides an important check of the validity of the relaxation model assumed in Sec. II. A formula for ω_{peak} in region I and the equation for the curve separating region I from region II in Fig. 2 are given in the Appendix.

We now examine the behavior of the cutoff frequency ω_c, where $\mathrm{Re}[\sigma(\omega, E_0)]$ drops to half its zero-frequency value. Contours of ω_c/Γ_{m0} as a function of $(dJ/dE)/(J/E)$ and G_e are shown in Fig. 6. The dashed line again separates regions I and II. The contours are seen to have only a weak dependence on the parameter G_e. For a given ω_c/Γ_{m0} and the range of the parameter G_e shown in Fig. 6, i.e., $0 < G_e < 6$, there is only a small interval within which $(dJ/dE)/(J/E)$ must lie. We use the contours of Fig. 6 to plot in Fig. 7 the permitted range of ω_c/Γ_{m0} (shaded region) for a given value of $(dJ/dE)/(J/E)$ and for $0 < G_e < 6$. If one considers larger values of G_e, then one can show that the contours of constant ω_c in Fig. 6 slowly but steadily decrease as $G_e \to \infty$. The result in Fig. 7 would be a lowering of the minimum possible ω_c/Γ_{m0} for a given $(dJ/dE)/(J/E)$. However, we expect $G_e < \sim 10$ and as ω_c varies slowly with G_e, Fig. 7 should provide reasonable bounds on ω_c for real materials.

Figure 7 suggests a second important consistency test that can easily be performed. For a nonlinear J versus E

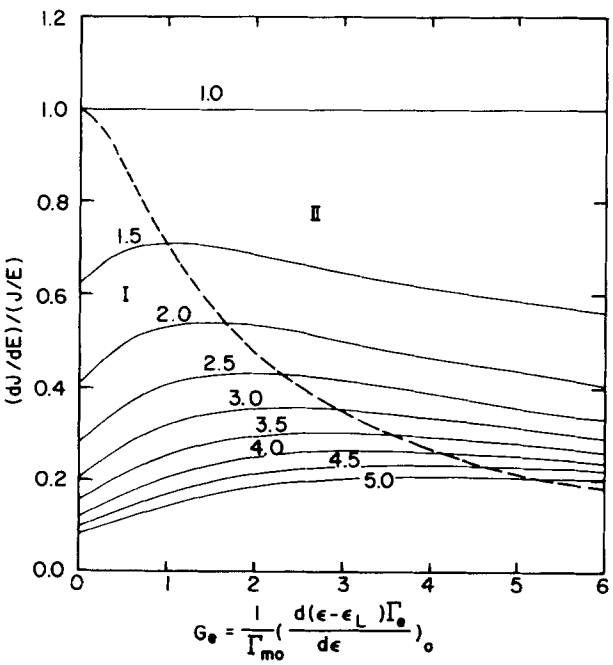

FIG. 6. Contours of cutoff frequency ω_c/Γ_{m0} (where $\mathrm{Re}[\sigma(\omega, E_0)]$ drops to half its $\omega = 0$ value) as a function of $(dJ/dE)/(J/E)$ and G_e. Below the dashed line corresponds to region I of Fig. 2, while region II of Fig. 2 lies above. Contours show no dramatic change as they pass from region I to region II.

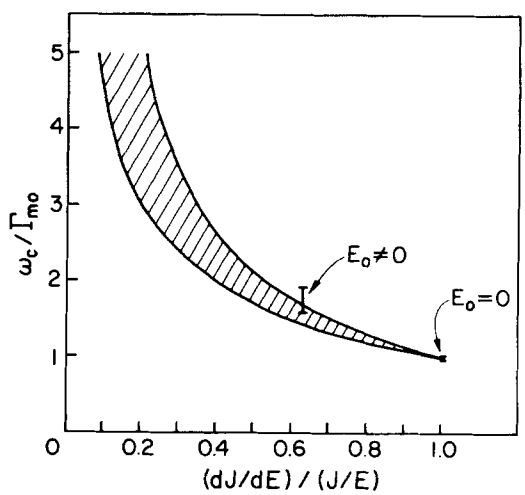

FIG. 7. Permitted range (shaded region) of cutoff frequency ω_c/Γ_{m0} for a given value $(dJ/dE)/(J/E)$ and $0 < G_e < 6$. Experimental results of Ref. 12 are indicated for one value of $E_0 \neq 0$ and for the $E_0 = 0$ case.

curve, the parameter $(dJ/dE)/(J/E)$ is easily controlled by varying the applied dc field E_0. Measurements of ω_c can therefore be made as a function of $(dJ/dE)/(J/E)$, and all points should lie within the shaded region of Fig. 7 if the model of Eq. (4) is to apply and G_e is not abnormally large. Recent experimental results of Allen *et al.*[12] for the cases $E_0 = 0$ (where $G_m = 0$ and $\omega_c/\Gamma_{m0} = 1$) and for one fixed value of $E_0 \neq 0$ are indicated in Fig. 7 and are seen to be consistent with our analysis.

IV. VELOCITY OVERSHOOT

We restate the intuitive argument for the existence of velocity overshoot as follows.[4] If $\Gamma_e \ll \Gamma_m$, we expect momentum relaxation to occur on time scales short compared to that on which the electron distribution heats up (i.e., system speeds up before it heats up). If the average electron energy is initially ϵ_i, then when an electric field E is turned on, the momentum will relax to give

$$v_i = \frac{qE}{m\Gamma_m(\epsilon_i)}. \tag{10}$$

At a larger time when the electrons have heated up to their final drift energy $\epsilon_f > \epsilon_i$, the momentum relaxes to give

$$v_f = \frac{qE}{m\Gamma_m(\epsilon_f)}. \tag{11}$$

If Γ_m is an increasing function of ϵ, then $v_i > v_f$ and overshoot has occurred.

We will now use the results of the previous sections to more rigorously examine the possibilities for overshoot in the case of a small field E_1 turned on at time $t = 0$ in the presence of a dc field E_0, i.e., $E(t) = E_0 + E_1\theta(t)$ [θ is the step function $\theta(t) = 0$ for $t < 0$, $\theta(t) = 1$ for $t > 0$]. From Sec. II we know the velocity response to an applied field of any frequency ω

$$v_1(\omega) = \mu(\omega, E_0)E_1(\omega), \tag{12}$$

where the mobility μ is related to the conductivity σ by

$$\mu = \sigma/nq. \tag{13}$$

Using the Fourier transform

$$\theta(t) = \int_{-\infty}^{\infty} \frac{d\omega}{2\pi i} \frac{e^{i\omega t}}{\omega - i\eta}, \tag{14}$$

(where η is an infinitesmally small positive number), we can easily obtain the velocity response to a step field as

$$v_1(t) = E_1 \int_{-\infty}^{\infty} \frac{d\omega}{2\pi i} \frac{e^{i\omega t}}{\omega - i\eta} \mu(\omega, E_0). \tag{15}$$

The behavior of $v_1(t)$ is thus completely determined by the poles of $\mu(\omega, E_0)$ and their residues.

Restricting ourselves to the same range of parameters as before, i.e., $|G_m| < G_e$ and $G_e > 0$, we have three possibilities. These are indicated by the regions shown in Fig. 8 and

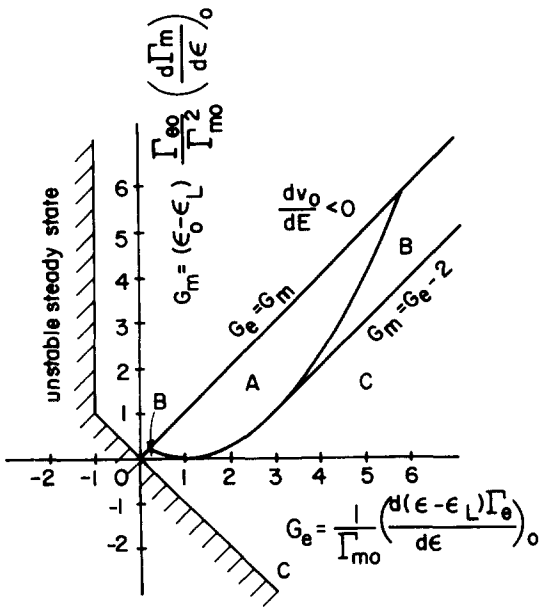

FIG. 8. Division of G_m, G_e parameter space according to behavior of velocity response to a small step field applied at $t = 0$. For points in region A, velocity overshoot occurs together with a small oscillation. For points in region B, overshoot occurs without oscillation. For points in region C, no overshoot occurs. Above the line $G_e = G_m$, there is negative differential mobility $dv_0/dE < 0$. To the left of the hatched line the steady state is unstable.

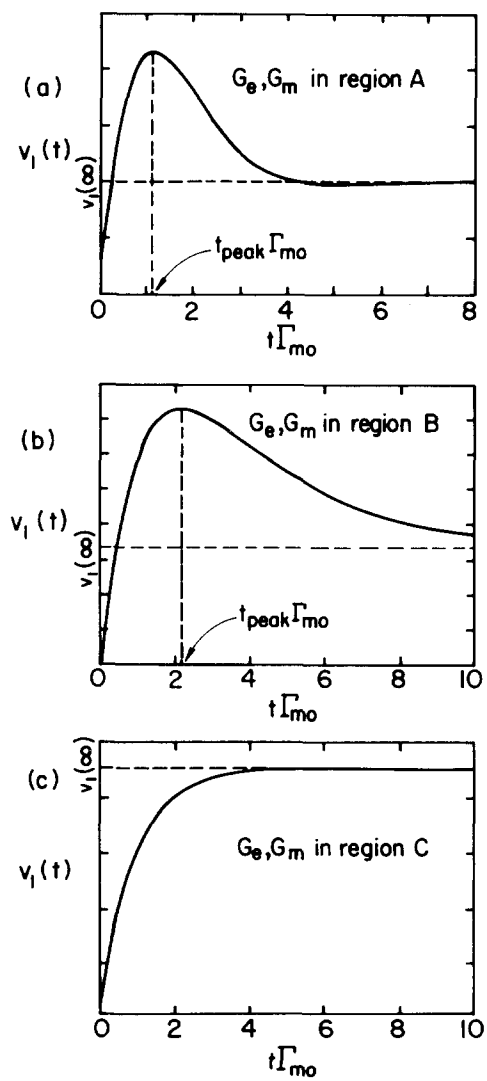

FIG. 9. Typical plots of velocity response $v_1(t)$ as a function of $t\Gamma_{m0}$: (a) corresponds to values of G_e and G_m in region A of Fig. 8, (b) corresponds to region B, and (c) corresponds to region C.

the corresponding behavior of $v_1(t)$ for each region, shown in Fig. 9. In region A, the poles of $\mu(\omega,E_0)$ are complex, and the resulting $v_1(t)$ displays overshoot with a small damped oscillation. In practice this oscillation will probably be too small to observe experimentally. In regions B and C, the poles are pure imaginary and $v_1(t)$ consists of a sum of pure exponentials. In region B, overshoot is present while in region C it is not.

Factorizing the denominator in Eq. (7) into a product of terms linear in ω gives for the poles of $\mu(\omega,E_0)$

$$\omega_{\pm} = i\left(\frac{1+G_e}{2}\right) \pm \left[-\left(\frac{1+G_e}{2}\right)^2 + G_e + G_m\right]^{1/2}. \quad (16)$$

From this, the equation for the line separating region A from regions B and C is obtained as

$$G_m = \left(\frac{G_e}{2}\right)^2 - \left(\frac{G_e}{2}\right) + \frac{1}{4}. \quad (17)$$

Consideration of when it is possible to have $dv/dt = 0$ for some finite t (this is the point of peak velocity) yields the equation for the lines separating the region of overshoot B from region C,

$$\begin{aligned} &G_m = 0 \quad \text{for } 0 < G_e < 1, \\ &G_m = G_e - 2 \quad \text{for } 3 < G_e. \end{aligned} \quad (18)$$

We can now compare these results with the intuitive argument presented at the beginning of this section. From Figs. 8 and 9 we see that no overshoot occurs if $G_m < 0$. This agrees with the intuitive assumption that $\Gamma_m(\epsilon)$, see (5a), must be an increasing function of ϵ. The second intuitive assumption that $\Gamma_e(\epsilon) \ll \Gamma_m(\epsilon)$ is less valid, but we may relate

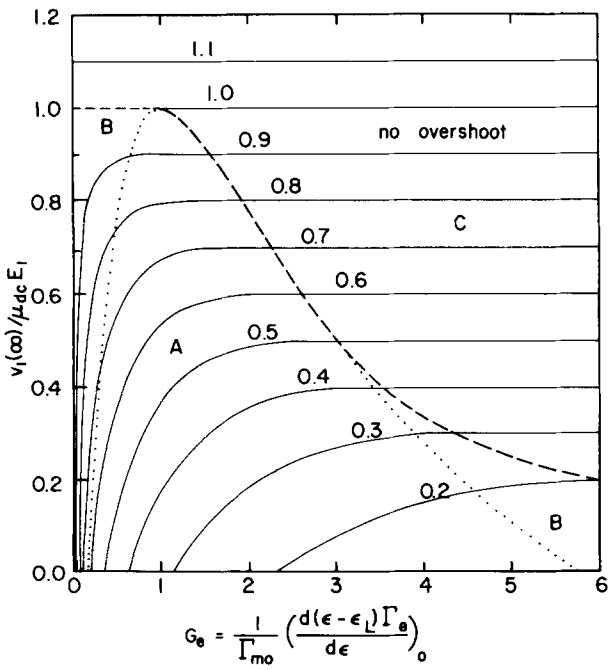

FIG. 10. Contours of peak velocity $v_1(t_{peak})/\mu_{dc}E_1$ as a function of $v_1(\infty)/\mu_{dc}E_1$ and G_e. Below the dashed line, overshoot is present while above it is not. Below the dotted line corresponds to region A of Fig. 8, while region B is between the dotted and dashed lines.

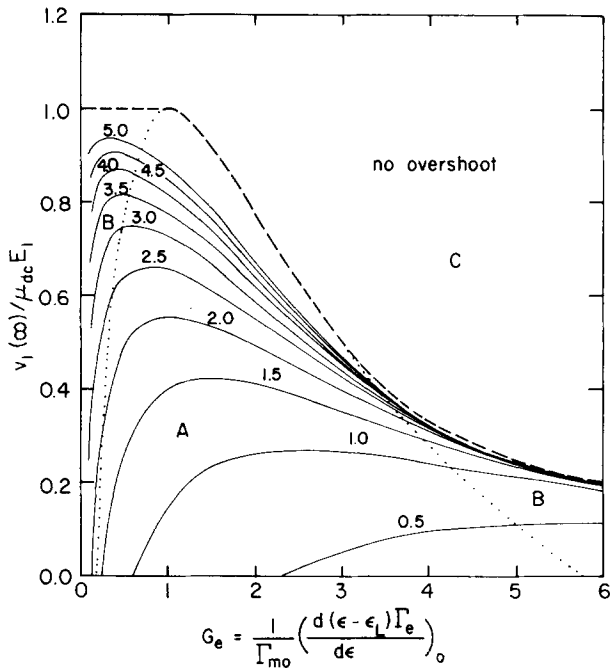

FIG. 11. Contours of time of peak velocity $t_{peak}\Gamma_{m0}$ as a function of $v_1(\infty)/\mu_{dc}E_1$ and G_e. Below the dashed line, overshoot is present while above it is not (i.e., $t_{peak} = \infty$). Below the dotted line corresponds to region A of Fig. 8, while region B is between the dotted and dashed lines.

it to our results as follows. If we assume that $\Gamma_e(\epsilon) \propto \Gamma_m(\epsilon)$ for all ϵ, there is a constant χ such that $\Gamma_e(\epsilon) = \chi\Gamma_m(\epsilon)$. Then from Eqs. (5) we would have $G_e = \chi + G_m$. From Eqs. (1) it may be shown that $\chi = 2$ corresponds to the case where $\epsilon(t) - \epsilon_L = (1/2)mv^2(t)$, and hence energy and momentum are relaxing together at the same rate. Thus the conduction $G_e - 2 < G_m$ would be equivalent to the condition $\Gamma_{e0} < 2\Gamma_{m0}$, and we have momentum relaxing faster than energy. Returning to Eq. (18) and Fig. 8, we see that the condition $G_e - 2 < G_m$ in fact must be satisfied in order for

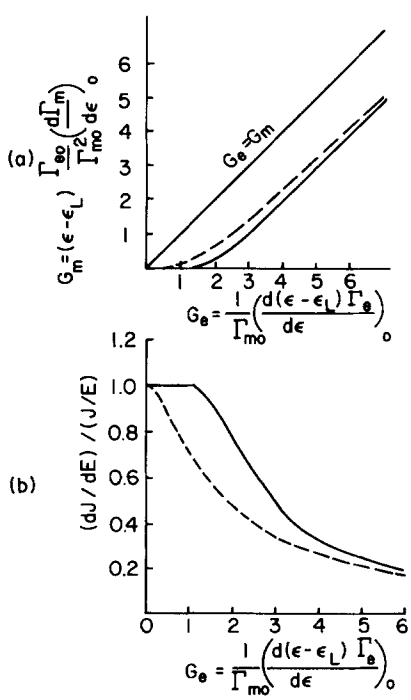

FIG. 12. Comparison of region where $\mathrm{Re}[\sigma(\omega,E_0)]$ has a peak at finite ω[(a) above dashed curve, (b) below dashed curve] with region where velocity overshoot exists[(a) above solid curve, (b) below solid curve]. Plot (a) is in the parameter space of G_m and G_e while plot (b) is in the parameter space of $(dJ/dE)/(J/E)$ and G_e. Observation of a peak conductivity at a finite frequency always implies the existence of overshoot; however, there is a small region (between the solid and dashed curves) where overshoot exists but the conductivity has no such peak.

overshoot to occur. However, the converse is not true. There remains a small region where both $G_m > 0$ and $G_e - 2 < G_m$, but overshoot is not present. Finally, of course, the condition $G_e - 2 < G_m$ need not imply $\Gamma_{e0} < 2\ \Gamma_{m0}$ when $\Gamma_e(\epsilon) \neq \chi \Gamma_m(\epsilon)$, as will generally be the case.

In Figs. 10 and 11 we plot contours of peak velocity $v_1(t_{\text{peak}})/(\mu_{\text{dc}} E_1)$ and the time of peak velocity $t_{\text{peak}} \Gamma_{m0}$ as functions of the long time-velocity increment $v_1(\infty)/(\mu_{\text{dc}} E_1) = (G_e - G_m)/(G_e + G_m)$ and G_e. The dashed line separates regions of velocity overshoot (i.e., regions A and B of Fig. 8) from that of no overshoot. The dotted line separates regions A and B. One sees that for a fixed value of G_e, the earlier the overshoot occurs, the bigger is the overshoot effect.

In Fig. 12 we compare the region of parameter space [in 12(a) as a function of G_m and G_e and in 12(b) as a function of $(dJ/dE)/(J/E)$ and G_e,] where one expects velocity overshoot, with the region where one expects a peak conductivity at a finite frequency. The latter region is seen to lie entirely within the former. We conclude that observation of a peak conductivity at a finite frequency is a sufficient condition to imply that the material will display velocity overshoot when operating at the same dc conditions. However, as the regions do not overlap exactly, velocity overshoot might still exist for materials whose conductivity does not have such a peak.

Finally, by comparing Fig. 12(b) with Fig. 6, we see that the cutoff frequency displays no dramatic change when we cross from the region of velocity overshoot to the region without. Thus the existence of velocity overshoot does not imply improved high-frequency performance of a material with uniform electron density. For devices where electron density is not uniform and device performance depends on the physical transfer of charge across low-density regions, velocity overshoot may still be an important means of improving high-frequency behavior.

V. CONCLUSIONS

In this paper we have applied a commonly used relaxation model to investigate ac conductivity and velocity overshoot phenomena. The response to small perturbations has been shown to depend entirely on just three parameters. We have indicated how these parameters may be easily extracted from dc and ac conductivity measurements and how such measurements may be used to check the validity of the relaxation model. The behavior of the ac conductivity as a function of the parameters of the theory has been explored by considering the magnitude of the peak conductivity, the frequency at which it occurs, and the cutoff frequency. Cutoff frequency has been shown to be dependent primarily upon the value $(dJ/dE)/(J/E)$ at the dc operating point.

We have derived precise restrictions on the energy and momentum relaxation rates for the occurrence of velocity overshoot in response to the addition of a small step field on top of an already existing dc field. These restrictions have been compared to more intuitive requirements presented previously, and qualitative though not quantitative agreement is found. It is shown that the occurrence of a peak in the ac conductivity at a finite frequency is a sufficient condition to imply the existence of velocity overshoot. Velocity overshoot is shown not to have any dramatic effect upon the cutoff frequency of the material.

ACKNOWLEDGMENTS

We would like to thank S. J. Allen and D. K. Ferry for useful conversations and correspondence. The hospitality of Nordita provided an opportunity for undisturbed collaboration. This work was supported by the Office of Naval Research.

APPENDIX

A formula for ω_{peak} in region I has been given previously.[7] In our notation it is

$$(\omega_{\text{peak}}/\Gamma_{m0})^2 = \frac{-B}{A} + \left[\left(\frac{B}{A}\right)^2 - \left(\frac{C}{A}\right)\right]^{1/2}, \tag{A1}$$

where

$$\begin{aligned} A &= 1 + G_m, \\ B &= G_e^2 - G_m^2, \\ C &= (G_e + G_m)[G_e^3 + G_m^2 - G_m(2 + 3\ G_e + G_e^2)]. \end{aligned} \tag{A2}$$

By noting that ω_{peak}^2 in Eq. (8) must be positive, we can derive the equation of the curve separating regions I and II as

$$G_m = \left(\frac{2 + 3\ G_e + G_e^2}{2}\right) - \left[\left(\frac{2 + 3\ G_e + G_e^2}{2}\right)^2 - G_e^3\right]^{1/2}. \tag{A3}$$

[1] E. M. Conwell, *Solid State Physics*, edited by F. Seitz, D. Turnbull, and H. Ehrenreich (Academic, New York, 1967), Suppl. 9.
[2] G. H. Glover, J. Appl. Phys. **44**, 1295 (1973).
[3] J. G. Ruch, IEEE Trans. Electron Devices **ED-19**, 652 (1972).
[4] T. J. Maloney and J. Frey, J. Appl. Phys. **48**, 781 (1977).
[5] H. Grubin in *Physics of Nonlinear Transport in Semiconductors*, edited by Ferry, Barker, and Jacoboni (Plenum, New York, 1980), p. 311.
[6] K. Blotekjaer, IEEE Trans. Electron Devices **ED-17**, 38 (1970).
[7] P. Das and D. K. Ferry, Solid-State Electron. **19**, 851 (1976).
[8] M. S. Shur, Electron. Lett. **12**, 615 (1976).
[9] Y. C. Wang, Phys. Status Solidi A **53**, K113 (1979).
[10] E. Rosencher, Solid State Commun. **38**, 1293 (1981).
[11] J. P. Nougier, J. C. Vaissiere, D. Gasquet, J. Zimmermann, and E. Constant, J. Appl. Phys. **52**, 825 (1981).
[12] S. J. Allen, D. C. Tsui, F. DeRosa, K. K. Thornber, and B. A. Wilson, J. Phys. Colloque **7**, C7-369 (1981).
[13] P. Das and R. Bharat, Appl. Phys. Lett. **11**, 386 (1967).
[14] P. N. Butcher, Rep. Prog. Phys. **30**, 97 (1967).